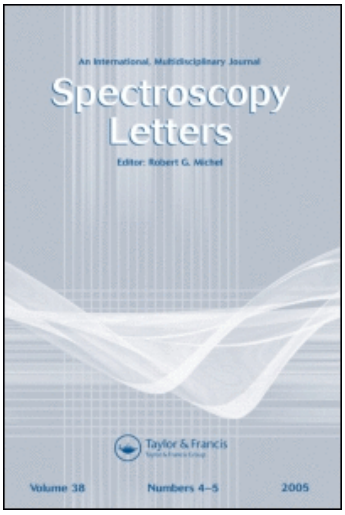

Spectroscopy Letters
Publication details, including instructions for authors and subscription information:
http://www.informaworld.com/smpp/title~content=t713597299

TOTAL ASSIGNMENT OF ^{1}H AND ^{13}C NMR SPECTRA OF A BRIDGED TRIRUTHENIUM CLUSTER-POLYPYRIDINE DIMER BASED ON 2D (COSY, HMQC, AND HMBC) TECHNIQUES

Sofia Nikolaou[a]; Miriam Uemi[a]; Henrique E. Toma[a]
[a] Instituto de Química, Universidade de São Paulo, São Paulo, SP, Brazil

Online publication date: 31 May 2001

To cite this Article Nikolaou, Sofia , Uemi, Miriam and Toma, Henrique E.(2001) 'TOTAL ASSIGNMENT OF ^{1}H AND ^{13}C NMR SPECTRA OF A BRIDGED TRIRUTHENIUM CLUSTER-POLYPYRIDINE DIMER BASED ON 2D (COSY, HMQC, AND HMBC) TECHNIQUES', Spectroscopy Letters, 34: 3, 267 — 277
To link to this Article: DOI: 10.1081/SL-100002281
URL: http://dx.doi.org/10.1081/SL-100002281

SPECTROSCOPY LETTERS, 34(3), 267–277 (2001)

TOTAL ASSIGNMENT OF ^{1}H AND ^{13}C NMR SPECTRA OF A BRIDGED TRIRUTHENIUM CLUSTER-POLYPYRIDINE DIMER BASED ON 2D (COSY, HMQC, AND HMBC) TECHNIQUES

Sofia Nikolaou, Miriam Uemi, and Henrique E. Toma*

Instituto de Química, Universidade de São Paulo, Caixa Postal 26077, CEP 05513-970, São Paulo, SP, Brazil

ABSTRACT

The bridged ruthenium cluster-polypyridine dimer $[Ru_3O(CH_3COO)_6(py)_2(tmbpy)Ru(bpy)_2(Cl)](PF_6)_2$ (py = pyridine, bpy = 2,2′-bipyridine and tmbpy = 4,4′-trimethylenedipyridine) has been synthesized and structurally characterized based on ^{1}H and ^{13}C NMR spectroscopy. This species exhibits a complex pattern of NMR signals due to the presence of a paramagnetic $[Ru_3O]$ core and seven non-equivalent aromatic rings. 2D NMR (COSY, HMQC and HMBC) correlation techniques have been required for the total assignment of the ^{1}H and ^{13}C NMR spectra.

Key Words: NMR; ^{1}H and ^{13}C correlation techniques; Modified trinuclear ruthenium clusters.

*Corresponding author.

INTRODUCTION

Trinuclear ruthenium clusters of the general formula $[Ru_3O(CH_3COO)_6(L)_3]^n$ have been extensively studied because of their relevant electrochemical and catalytic properties. These properties arise from the triangular structure in which the three interacting ruthenium ions are held together by μ-oxo and μ-acetate bridges. NMR spectroscopy has provided a powerful tool in the structural characterization of this type of compound (1); however, along the last 20 years the assignment has been carried out exclusively on a comparative basis (1–8). Recently, by using correlation techniques, it was shown that ^{13}C assignments carried out in parallelism with the ^1H NMR data, can be misleading (9).

The difficulties of interpreting the NMR spectra increase dramatically in the case of multi-bridged species containing metal-organic fragments, such as the $[Ru_3O(CH_3COO)_6(py)_2(tmbpy)Ru(bpy)_2(Cl)]^{2+}$ (py = pyridine, bpy = 2,2-bipyridine and tmbpy = 4,4′-trimethylenedipyridine) complex (Figure 1) reported in this work. The complete assignment of the ^1H and ^{13}C NMR spectra of this novel species was pursued, aiming its structural characterization, based on 2D (COSY, HMQC and HMBC) correlation techniques.

RESULTS AND DISCUSSION

The dimer exhibits a large number of peaks in the ^1H and ^{13}C NMR spectra, as shown in Figures 1 and 2, as a consequence of the non equivalence of the aromatic rings (except the two pyridine ligands). In addition, as one can see in Figure 1, the ring labeled (2-3-4-5-6) should exert direct influence (from ring current effects) onto proton **10**; the (7-8-9-10-11) ring should affect the proton **6′** signal and the (α_2-β_2-γ_2) ring in the bridging ligand should affect proton **6**. In the bridging 4,4′-trimethylenebipyridine ligand (tmbpy), the rings are non-equivalent since the (α_1-β_1-γ_1) ring is subjected to the paramagnetic anisotropy of the $[Ru_3O]$ core, as well as the peripheral pyridine rings.

The assignment of the ^1H signals was carried out from COSY measurements, as shown in Figure 3, where it is illustrated all the correlations expected for the whole molecule.

Analogously, most of the ^{13}C could be assigned from the HMQC spectrum shown in Figure 4, except the quaternary carbons and the bridging ligand carbons which will be discussed later.

The complete ^1H and ^{13}C data are shown in Tables 1 and 2, respectively. As one can see, the δ values of the $[Ru(bpy)_2]$ moiety protons follow the same pattern observed for the $[Ru(bpy)_3]^{2+}$ complex (10,11). Due to coordination to ruthenium, the free rotation of the bpy rings is not possible. In addition, the protons **3**, **3′**, **7** and **7′** are sterically strained, in such a way that the Van der Waals interaction

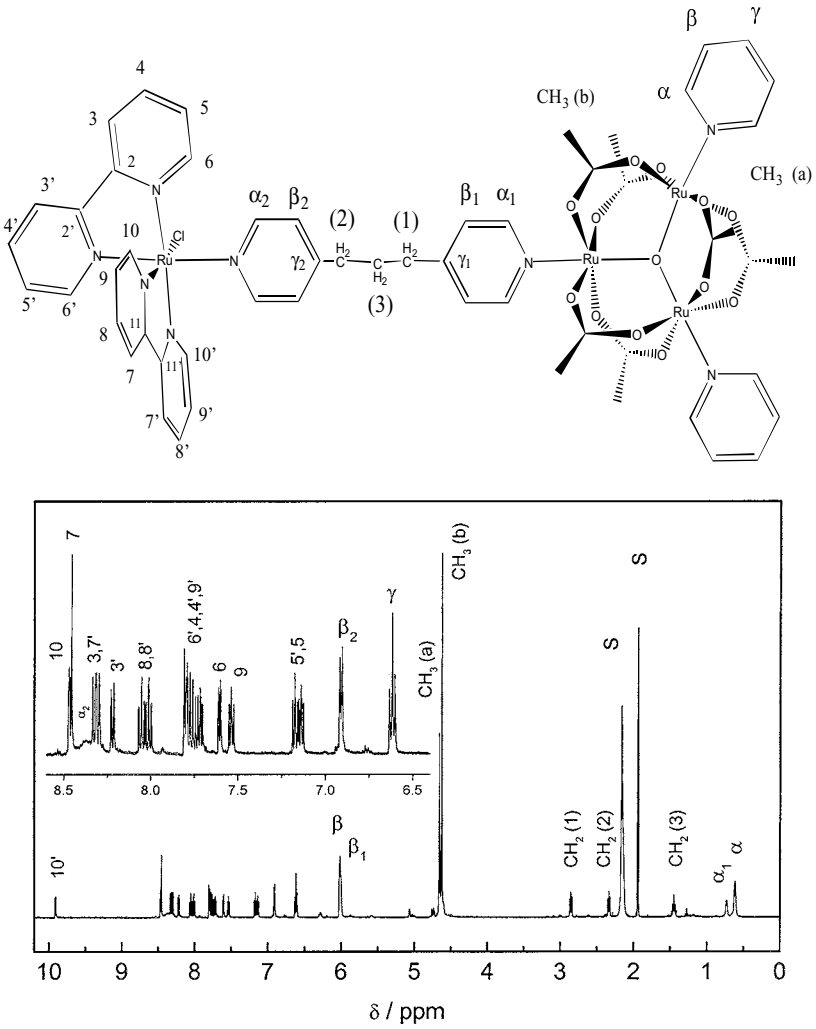

Figure 1. Structural representation of the dimer $[Ru_3O(CH_3COO)_6(py)_2(tmbpy)Ru(bpy)_2(Cl)](PF_6)_2$ and its ^{1}H NMR spectrum in CD_3CN solution. (S = solvent peak; inset = expanded spectrum).

between them causes a deshielding effect, shifting their signals to lower field in relation to other protons of that ligand (11). An interesting feature is the doublet signal at 9.89 ppm, assigned to proton **10′**. This large shift to lower field has also been observed in other mononuclear ruthenium complexes. It arises from the close proximity of that proton to the adjacent Cl^- ion, and has been attributed to inductive

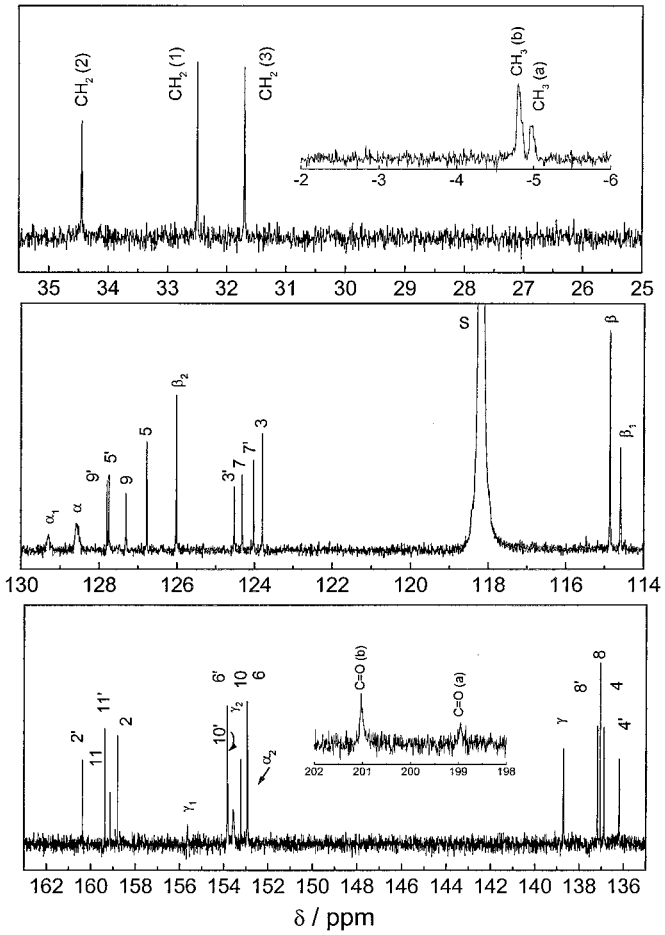

Figure 2. Expanded segments of ^{13}C NMR spectrum of the dimer $[Ru_3O(CH_3COO)_6(py)_2(tmbpy)Ru(bpy)_2(Cl)](PF_6)_2$ in CD_3CN solution. S = solvent peak.

effects from that ion (12,13). Protons **6**, **6′** and **10** are subjected to *ring current* effects. These protons are located in the shielding region of the bpy aromatic rings and therefore have their signals shifted to higher field in relation to free ligand. As expected, protons **5**, **5′**, **9**, and **9′** appear as triplets with values of δ varying from 7.13 ppm to 7.71 ppm due to the non-equivalence of the bpy rings. The same discussion can be done for protons **4**, **4′**, **8** and **8′**, except that the signals of **4**, **4′** are superimposed.

In general, the ^1H δ values of the $[Ru_3O(CH_3COO)_6(py)_2]$ unit are comparable with the corresponding values observed for the monomeric cluster

MARCEL DEKKER, INC.
270 Madison Avenue, New York, New York 10016

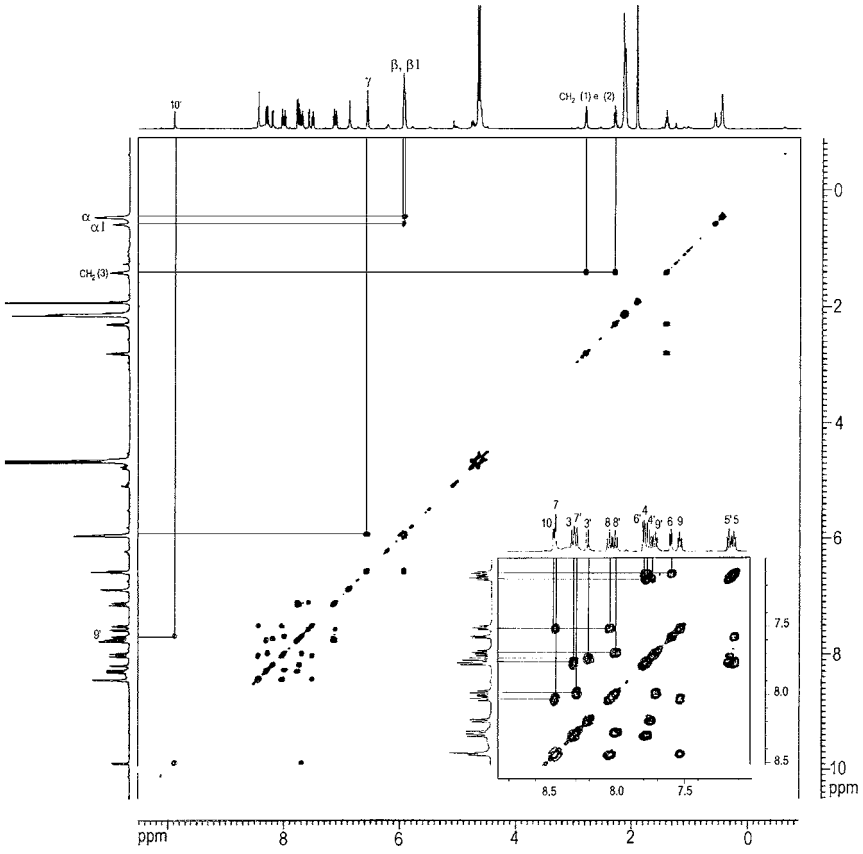

Figure 3. (^{1}H - ^{1}H) COSY plots for the dimer $[Ru_3O(CH_3COO)_6(py)_2(tmbpy)Ru(bpy)_2(Cl)](PF_6)_2$ in CD_3CN solution.

$[Ru_3O(CH_3COO)_6(py)_2(tmbpy)]PF_6$ (Table 1). In the case of the bridging ligand, one can observe significant shifts in ^{1}H δ values, specially for the ring directly coordinated to the $[Ru_3O]$ center; this effect is less pronounced for the second ring, bound to the diamagnetic Ru^{II} ion (see structure in Figure 1). The assignment of the carbon chain protons was made based on the correlations observed in the HMQC spectra, after the ^{13}C assignment based on the HMBC spectra (Figures 4A and 4B, respectively).

The δ value of proton α_1 shows a large shift to higher field in relation to free ligand, i.e. 0.63 ppm and 8.51 ppm respectively. The magnitude of the shifts decreases with distance, being smaller for proton β_1, (CH_2) groups, β_2 and finally α_2. Protons of the py ligand present the same trend of shifts to higher field. This

MARCEL DEKKER, INC.
270 Madison Avenue, New York, New York 10016

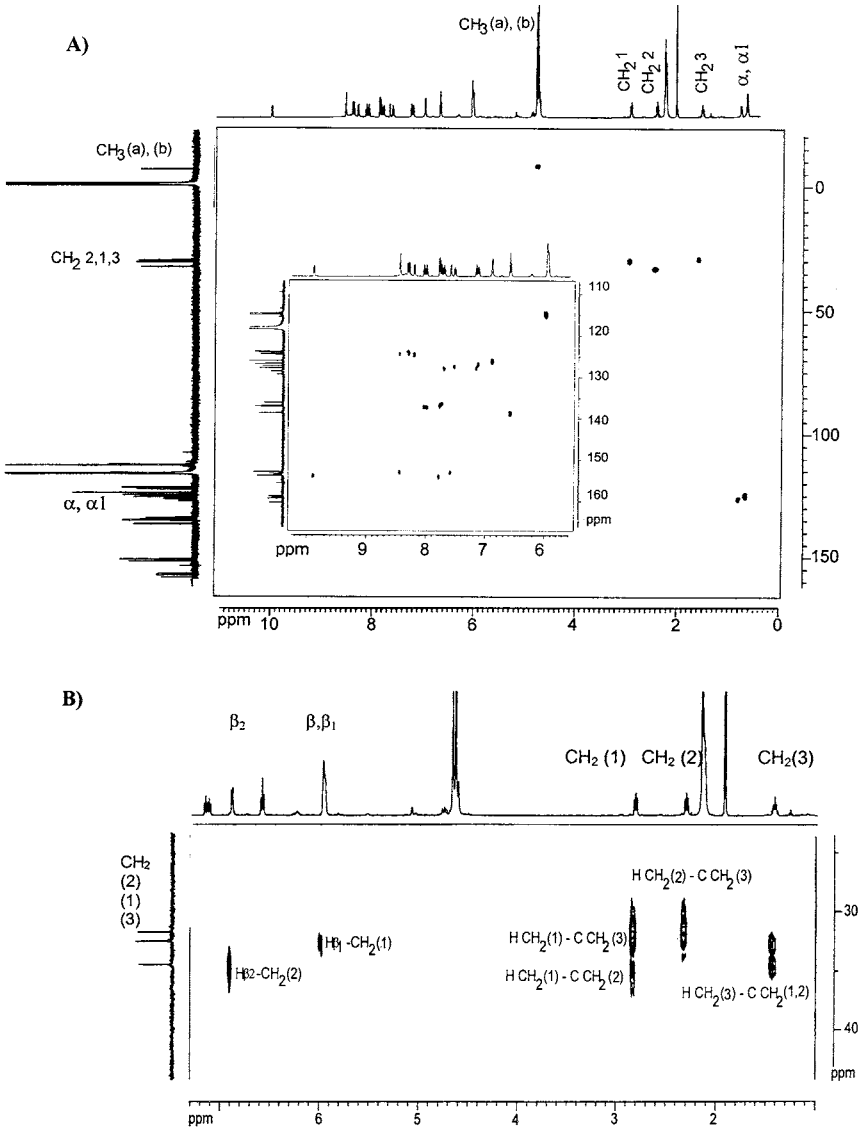

Figure 4. (^{1}H - ^{13}C) HMQC plots for the dimer $[Ru_3O(CH_3COO)_6(py)_2(tmbpy)Ru(bpy)_2(Cl)](PF_6)_2$ (a) and a selected region of the (^{1}H - ^{13}C) HMBC spectrum used to assign the carbon chain of the bridging ligand (b) in CD_3CN solution.

MARCEL DEKKER, INC.
270 Madison Avenue, New York, New York 10016

Table 1. ^{1}H NMR Chemical Shifts (ppm) for the Dimer $[Ru_3O(CH_3COO)_6(py)_2(tmbpy)Ru(bpy)_2(Cl)](PF_6)_2$ in CD_3CN

Proton	δ(ppm)	Free Ligand[a]	$[Ru_3O(Ac)_6(py)_2(tmbpy)]^{+(b)}$	$[Ru(bpy)_3]^{+2(c)}$
			Pyridine	
H_α	0.51	8.6	0.35	*
H_β	5,98	7.2	5.88	*
H_γ	6,59	7.6	6.57	*
			Acetate	
CH_3(a)	4,68	2.1	4.69	*
CH_3(b)	4,65	2,1	4.68	*
			4,4'-Trimethylenedipyridine	
$H\alpha_1$	0.63	8.51	0.43	*
$H_{\beta 1}$	5.96	7.10	5.93	*
CH_2 (1)	2.82	2.65	2.82	*
CH_2 (2)	2.32	2.65	2.36	*
CH_2 (3)	1.43	1.99	1.48	*
H_{β_2}	6.89	7.10	7.03	*
$H\alpha_2$	8.37	8.51	8.33	*
			2,2′-Bipyridine	
H_3	8.31	8.42	*	8.83
$H_{3'}$	8.21	8.42	*	8.83
H_7	8.44	8.42	*	8.83
$H_{7'}$	8.29	8.42	*	8.83
H_4	7.78	7.77	*	8.23
$H_{4'}$	7.75	7.77	*	8.23
H_8	8.04	7.77	*	8.23
$H_{8'}$	8.00	7.77	*	8.23
H_5	7.13	7.25	*	7.59
$H_{5'}$	7.16	7.25	*	7.59
H_9	7.53	7.25	*	7.59
$H_{9'}$	7.71	7.25	*	7.59
H_6	7.59	8.67	*	8.07
$H_{6'}$	7.79	8.67	*	8.07
H_{10}	8.46	8.67	*	8.07
$H_{10'}$	9.89	8.67	*	8.07

[a]Data from the SADTLER RESEARCH LABORATORIES collection.
[b]Data obtained in our laboratory.
[c]Data from reference 11.

MARCEL DEKKER, INC.
270 Madison Avenue, New York, New York 10016

Table 2. ^{13}C NMR Chemical Shifts (ppm) for the Dimer $[Ru_3O(CH_3COO)_6(py)_2(tmbpy)Ru(bpy)_2(Cl)](PF_6)_2$ in CD_3CN

Carbon Atom	δ (ppm)	Free Ligand[a]	Carbon Atom	δ (ppm)	Free Ligand[a]
Pyridine			4,4′Trimethylenedipiridine		
C_α	128.55	149.9	$C_{\alpha 1}$	129.28	149.8
C_β	114.84	123.7	$C_{\beta 1}$	114.57	123.8
C_γ	138.69	135.7	$C_{\gamma 1}$	155.63	150.4
Acetate			CH_2 (1)	32.48	34.3
			CH_2 (3)	31.67	30.4
CH_3 (a)	−5.00	20.7	CH_2 (2)	34.42	34.3
CH_3 (b)	−4.82	20.7	$C_{\gamma 2}$	153.54	150.4
C=O (a)	198.93	177.7	$C_{\beta 2}$	125.99	123.8
C=O (b)	201.00	177.7	$C_{\alpha 2}$	152.92	149.8
*	*	*			
2,2′-Bipyridine					
C_2	158.78	156.2	C_8	137.04	136.7
$C_{2'}$	160.36	156.2	$C_{8'}$	137.16	136.7
C_{11}	159.36	156.2	C_5	126.75	121.0
$C_{11'}$	159.11	156.2	$C_{5'}$	127.73	121.0
C_3	123.78	123.5	C_9	127.29	121.0
$C_{3'}$	124.49	123.5	$C_{9'}$	127.78	121.0
C_7	124.29	123.5	C_6	152.93	149.1
$C_{7'}$	124.00	123.5	$C_{6'}$	153.83	149.1
C_4	136.86	136.7	C_{10}	153.22	149.1
$C_{4'}$	136.18	136.7	$C_{10'}$	153.80	149.1

[a]Data from the SADTLER RESEARCH LABORATORIES collection.

fact can be explained in terms of the paramagnetic anisotropy of the $[Ru_3O]$ core, which contains one unpaired electron (1). This effect can operate through two mechanisms. The first one is called pseudocontact or dipolar interaction (14), and involves a dipolar interaction through space that decreases with distance. However it depends on the orientation of the observed nucleus and the paramagnetic center, making it possible to observe shifts either to high or down field. This explains why the α and α_1 protons show the largest shifts and also the fact that the methyl acetate protons are downfield shifted (Table 1), following an opposite trend to that observed for the pyridine protons. Another aspect to be noted is the broadening of the proton and even carbon signals at α and α_1 positions. Finally, the observed splitting of the signals for the methyl (acetate) groups was expected since there are

MARCEL DEKKER, INC.
270 Madison Avenue, New York, New York 10016

two magnetically non-equivalent types of acetate: four *vicinal* and two in *trans*-position with respect to the bridging ligand.

A similar discussion can be done concerning the δ values observed for the ^{13}C atoms in the $[Ru_3O(CH_3COO)_6(py)_2]$ unit, which are also strongly influenced by the paramagnetic effect. However, it is interesting to note that the proton and carbon atoms of the methyl (acetate) groups, follow opposite trends. This can be rationalized in terms of the second mechanism of paramagnetic interaction, the Fermi contact mechanism (14). The interaction involves a polarization of nearby electrons by the unpaired one (spin polarization), which propagates through bonds, alternating the influence on the chemical shifts of bound carbons and protons.

The assignment of the quaternary carbons was carried out from the HMBC measurement. The γ_1 and γ_2 carbons of the bridging ligand were unequivocally assigned in accord to the J_2 and J_3 correlations with CH_2 (1, 2) and CH_2 (3) respectively. Carbons **2** and **2′** were assigned from the J_2 and J_3 correlations with the corresponding H (3, 3′) and H (4, 4′; 6, 6′) respectively. Finally, carbons **11** and **11′** were assigned from the J_2 and J_3 correlations with protons H (7, 7′) and H (**10**; **8**, **8′**) respectively.

As a final remark, by focusing on a relatively complex cluster-ruthenium polypyridine species, this work has illustrated the great usefulness of the 2D techniques on allowing its structural characterization, and provided, on the other hand, an interesting view of the several electronic and magnetic influences in the molecule.

EXPERIMENTAL

The synthetic method employed in the preparation of asymmetric clusters such as $[Ru_3O(CH_3COO)_6(py)_2(tmbpy)]PF_6$ (shown here for comparison purposes) is reported elsewhere (1). The synthesis of the dimer was carried out by reacting stoichiometric amounts of the precursors $[Ru_3O(CH_3COO)_6(py)_2(CH_3OH)]PF_6$ and $[Ru(bpy)_2(tmbpy)(Cl)]PF_6.H_2O$ in CH_2Cl_2 during 48 h, at room temperature, in the dark. The crude product was purified by chromatography through neutral alumina, using a 1:1 mixture of CH_2Cl_2 and CH_3CN. Found: C, 36.5; H, 3.5; N, 6.1. $[Ru_3O(CH_3COO)_6(C_5H_5N)_2Ru(C_{10}H_8N_2)_2(C_{13}H_{14}N_2)(Cl)](PF_6)_2$ requires C, 36.6; H, 3.4; N, 6.3.

The ^{1}H NMR spectrum of the cluster $[Ru_3O(CH_3COO)_6(py)_2(tmbpy)]PF_6$ was recorded on a Varian 300MHZ spectrometer, model INOVA 1 at room temperature; all the other NMR spectra (^{1}H,^{13}C, ^{1}H-^{1}H COSY, ^{1}H-^{13}C HMQC and ^{1}H-^{13}C HMBC) were recorded on a Brucker DRX 500MHz spectrometer. The measurements were carried out at 305K, using 10^{-2} mol dm^{-3} solutions in CD_3CN. The

signals are reported to the residual protons of solvent. COSY was recorded using 2s as relaxation delay and spectral width (sw) of 6983Hz; in HMQC was used a relaxation delay of 1.5s and sw=126500Hz (f_1 dimension$-^{13}C$) and sw=7003Hz (f_2 dimension - ^1H); The pulse sequence of HMBC measurement was 2s, 3.45 and 62.5ms (D1, D2 and D6 delays) and sw=126500Hz (f_1 dimension - ^{13}C) and sw = 6983Hz (f_2 dimension $-$ ^1H). (Additional material for consult purposes is available under request).

ACKNOWLEDGMENTS

The financial support from John Simon Guggenheim Memorial Foundation (HET), and the Brazilian Agencies FAPESP and CNPq, is gratefully acknowledged.

REFERENCES

1. Baumann J. A., Salmon D. J., Wilson S. T., Meyer T. J., Hatifield W. E. Electronic Structure and Redox Properties of the Clusters $[Ru_3O(CH_3CO_2)_6(L_3)]^{n+}$. Inorg. Chem. 1978; 17:3342.
2. Walsh J. L., Baumann J. A., Meyer T. J. Rate of Self-Exchange between the Delocalized Clusters $[Ru_3O(CH_3CO_2)_6(py)_3]^{+/0}$. Inorg. Chem. 1980; 19:2145.
3. Sasaki Y., Tokiwa A., Ito T. Mixed Ruthenium-Rhodium Trinuclear Complex $[Ru_2Rh(\mu_3\text{-}O)(\mu\text{-}CH_3COO)_6(L)_3]^+$ (L=H_2O or Pyridine). J. Am. Chem. Soc. 1987; 109:6341.
4. Toma H. E., Alexiou A. D. P., Nuclear Magnetic Resonance and Spectroelectrochemical Characterization of a Supramolecular Tetrameric Ruthenium Cluster. J. Chem. Research (S) 1995; 134.
5. Toma H. E., Alexiou A. D. P., Synthesis and Characterization of a Dodecanuclear Ruthenium Pyrazine Cluster. J. Braz. Chem. Soc. 1995; 6:267.
6. Abe M., Sasaki Y., Yamada Y., Tsukahara K., Yano S., Yamaguchi T., Tominaga M., Taniguchi I., Ito T. Oxo-Centered Mixed-Ligand Triruthenium Complexes Having Redox-Active *N*-Methyl-4,4′-bipyridinium Ions ($mbpy^+$). Reversible Multistep Electrochemical Properties of $[Ru^{III}_2Ru^{II}(\mu_3\text{-}O)(\mu\text{-}CH_3CO_2)_6(mbpy^+)_2(CO)]^{2+}$ and $[Ru^{III}_3(\mu_3\text{-}O)(\mu\text{-}CH_3CO_2)_6(mbpy^+)_2(CL)]^{3+}$ (L=H_2O and *N*-Heterocyclic Ligands). Inorg. Chem. 1996; 35:6724.
7. Alexiou A. D. P., Toma H. E. NMR Spectroscopic Correlations for a Series of Triangular μ-Oxoruthenium Acetate Clusters containing Substituted Pyridine Ligands. J. Chem. Research (S) 1997; 338.

MARCEL DEKKER, INC.
270 Madison Avenue, New York, New York 10016

8. Ota K., Sasaki H., Matsui T., Hamaguchi T., Yamaguchi T., Ito T., Kido H., Kubiak C. P. Synthesis and Properties of a Series of Oxo-Centered Triruthenium Complexes and Their Bridged Dimers with Isocyanide Ligands at Terminal and Bridging Positions. Inorg. Chem. 1999; 38:4070.
9. Toma H. E., Alexiou A. D. P., Nikolaou S., Dovidauskas S., ^{13}C NMR Spectra of Triangular μ-oxoruthenium Acetate Clusters Revisited: HETCOR Study of Two Pyridine and 4,4′-bipyridine Derivative. Magn. Reson. Chem. 1999; 37:322.
10. Constable E. C., Seddon K. R. A Deuterium Exchange Reaction of the Tris-(2,2′-bipyridine)ruthenium(II) Cation: Evidence for the Acidity of the 3,3′-Protons. J. Chem. Soc., Chem. Commun. 1982; 34.
11. Constable E. C., Lewis J. NMR Studie on Ruthenium(II) α,α'-Diimine Complexes; Further Evidence for Unique Reactivity at $H_{3,3'}$ of Coordinated 2,2′-Bipyridines. Inorg. Chim. Acta 1983; 70:251.
12. Leising R. A., Kubow S. A., Churchill M. R., Buttrey L. A., Ziller J. W., Takeuchi K. J. Synthesis, Characterization, and X-ray Crystal Structure of $[Ru(NO_2)(PMe_3)_2(trpy)](ClO_4)$. Inorg. Chem. 1990; 29:1306.
13. Heijden M., van Vliet P. M., Haasnoot J. G., Reedijk J. Synthesis and Characterization of *cis*-(2,2′-Bipyridine)(2,2′-Biquinoline) dichlororuthenium(II) and its Co-ordination Chemistry with Imidazole Derivatives. J. Chem. Soc. Dalton Trans. 1993; 3675.
14. Bertini I., Luchinat C. NMR of Paramagnetic Substances. Coord. Chem. Rev. 1996; 150:1.

Received September 25, 2000
Accepted December 15, 2000

Request Permission or Order Reprints Instantly!